Journal of Alloys and Compounds 509 (2011) 6414–6417

Contents lists available at ScienceDirect

Journal of Alloys and Compounds

journal homepage: www.elsevier.com/locate/jallcom

Synthesis and ageing effect in FeO nanoparticles: Transformation to core–shell FeO/Fe_3O_4 and their magnetic characterization

S.K. Sharma [a,*], J.M. Vargas [b], K.R. Pirota [a], Shalendra Kumar [c], C.G. Lee [c], M. Knobel [a]

[a] Instituto de Fisica Gleb Wataghin, Universidade Estadual de Campinas (UNICAMP), Campinas 13.083-859, SP, Brazil
[b] Advanced Materials Research Institute, University of New Orleans, New Orleans, LA 70148 USA
[c] School of Nano & Advanced Materials Engineering, Changwon National University, 9 Sarim dong, Changwon 641-773, South Korea

ARTICLE INFO

Article history:
Received 6 December 2010
Received in revised form 8 March 2011
Accepted 10 March 2011
Available online 21 March 2011

PACS:
81.16.Be
87.85.Rs
75.50.Tt
75.75. +a
75.30.Gw

Keywords:
Chemical synthesis
Colloidal nanoparticles
Superparamagnetism
Core–shell nanoparticles
Magnetite
Wüstite

ABSTRACT

This paper reports the magnetic properties of partially oxidized FeO nanoparticles (NPs) prepared using thermal decomposition of iron acetylacetonate at high temperature. X-ray diffraction (XRD) analysis confirmed that the resulting NPs comprise a mixture of wüstite and magnetite phases, which are subsequently confirmed using high resolution transmission electron microscopy (HR-TEM) and selected area electron diffraction (SAED) pattern. Magnetic properties were investigated using vibrating sample magnetometer (VSM), which exhibit superparamagnetic (SPM) behavior at room temperature. Alternatively, below 200 K, a large exchange bias field has been observed in field cooled mode whose magnitude increases with the decrease in measuring temperature attaining a maximum value of ~2.3 kOe at 2 K accompanied by coercivity enhancement (~3.4 kOe) and high field of irreversibility (>50 kOe). The results are discussed taking into account the role of interface exchange coupling on the macroscopic magnetic properties of the nanoparticles.

1. Introduction

Magnetic iron oxide based nanoparticles (NPs) have become the center of attraction among the scientific community because of their increasing number of applications in various fields [1]. Recently, much attention has been paid towards the wüstite (FeO) NPs not because of their complex magnetic structure, but also their interesting defect related magnetic properties [2,3]. In addition to this, they show interesting phase transformation to multiphase nanostructures with fascinating and superior magnetic properties, for example, exchange bias (EB) accompanied by an enhancement of coercivity after field cooling through Néel temperature (T_N) of antiferromagnetic (AFM). EB was first reported in colloidal magnetic NPs system composted of Co partially oxidized [4] and extensive research followed this discovery to understand this effect and ideally to control it for further technological applications. Numerous applications of EB exist in present technologies, such as spin valves and magnetic tunnel junction [5] and it is being considered as a possible way to overcome the superparamagnetic (SPM) limit for the magnetic storage [6].

Although there has been some research on EB in granular materials in the last decades [7–12], but the majority of research has focused mainly on thin film systems [13–17]. This is mostly because the spin distribution in granular systems particularly core–shell NPs are essentially more intricate than that of thin films. Additionally, the particle size distribution and tendency of particles to aggregate in solution also make quantitative measurements more complicated [18]. Nevertheless, recent advances in magnetic NPs production by chemical routes have propelled a renewed interest in granular nanostructures exhibiting EB. Bianco et al. [19] studied the EB properties of a granular system composed of Fe NPs embedded in a Fe-oxide host, where they observed variations that were explained in terms of interfacial exchange coupling between a ferromagnetic phase (the Fe NPs) and the disordered magnetic phase (the Fe-oxide host). Besides being found in FM/AFM bilayers and nanoparticulate systems, the EB was observed in inverted core–shell MnO/Mn_3O_4, FeO/Fe_3O_4, antiferromagnets and ferrimagnets (FiM) such as CuO, NiO and Fe_3O_4, $NiFe_2O_4$ as well as in

* Corresponding author.
E-mail address: surender76@gmail.com (S.K. Sharma).

0925-8388/$ – see front matter © 2011 Elsevier B.V. All rights reserved.
doi:10.1016/j.jallcom.2011.03.072

some spin glasses [20–23]. Recently, Chen et al. [3] have studied the time evolution of EB properties in monodisperse wüstite NPs prepared via thermal decomposition of iron (III) oleate complex at 380 °C using oleic acid as solvent. These developments have kindled interests to broaden this approach to further study the effect of time evolution on EB behavior and the stability of core–shell structure in partially oxidized wüstite NPs. Here, we report a simple recipe as described by Hou et al. [2] for the preparation of spherical wüstite (FeO) NPs with some minor modifications, but completely different from Chen et al. [3]. The stability of the obtained NPs has been checked after a regular interval of time under ambient conditions. It was found that even after 125 days the NPs still exhibit FeO/Fe_3O_4 core–shell structure along with a large EB below T_N, accompanied by enhancement in the coercive force.

2. Experimental details

In a typical synthesis to prepare FeO NPs, iron (III) acetylacetonate [$Fe(acac)_3$] (2 mmol) is mixed with 20 ml of 1-octadecene, 8 ml of oleyamine (27 mmol) and 8 ml of oleic acid (25 mmol) at room temperature (keeping the molar ratio of Fe/surfactant = 1:26). The mixture was gently heated at 120 °C for 45 min under continuous Ar flux with intermediate stirring. The above mixture was heated at 310 °C for 60 min under Ar flux with heating rate of ~5 °C/min. Finally, the solution was cooled down to room temperature. The NPs were washed adding access of ethanol and centrifugation at 3800 rpm for 10 min. This procedure was repeated 3–4 times by dispersing the NPs in toluene, adding excess of ethanol and centrifugation. Finally, the NPs were dispersed in toluene (concentration of 0.05 g/ml) for long-term storage. Hereby the NPs remain coated with surfactant. The above procedure gave originally FeO NPs as confirmed by x-ray diffraction (XRD) followed by a core–shell structure of size ~25 nm of FeO/Fe_3O_4 under ambient conditions for more than 125 days. These particles were then investigated thoroughly and their magnetic properties were studied on the basis of core–shell internal structure.

The particle diameter and its distribution were measured by means of transmission electron microscopy (TEM) (300 keV JEM 3010 microscope) at Brazilian Synchrotron Light Laboratory (LNLS) by drying a toluene dispersion of the NPs on a carbon coated copper grid and allowing it to dry. The structure was determined by XRD (Philips, X-PERT) with Cu K_α radiations and the magnetic properties were measured on dried powder sample using PPMS (Quantum Design) magnetometer installed with VSM option with fields up to 140 kOe and temperatures from 2 to 350 K.

3. Results and discussion

Fig. 1(a and b) shows the typical TEM images for the FeO/Fe_3O_4 NPs sample along with histogram of size distributions, which was built up by counting of more than 200 particles and fitted with a Gaussian distribution (full-line), resulting in an average diameter of 25 nm and distribution width of ±3.0. It is found in the images (see Fig. 1(a)) that most of the particles show an inner contrast variation suggesting the existence of core–shell structure. In addition to this, we have also observed the absence of such a contrast variation in some of the particles which could be explained by complete oxidation of those particles during the washing process or thereafter. The corresponding HR-TEM image of particles shows that it is highly crystallized as indicated by apparent atomic lattice fringes (see Fig. 1(b)). The observed lattice fringes are distributed consistently inside the single particle with d_{111} = 0.479 nm, assigned to Fe_3O_4. Selected area electron diffraction (SAED) was also performed in order to further strengthen the above observations and the corresponding pattern is shown in Fig. 1(c). The interplanar distance of each electron diffraction ring was carefully quantified and the results show that the rings composed of mixture of Fe_3O_4 and FeO

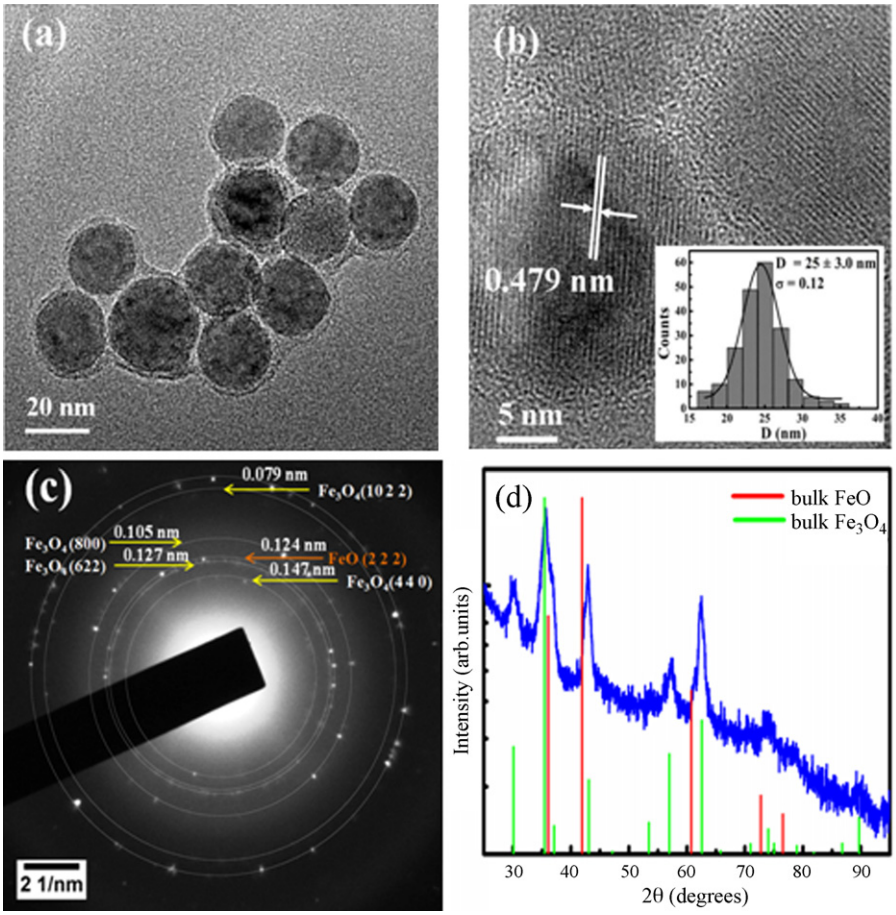

Fig. 1. (a and b) HR-TEM image for FeO/Fe_3O_4 core–shell NPs, (c) SAED pattern, which shows the mixed spinel Fe_3O_4 and wüstite phase, and (d) XRD pattern for the same sample.

phases. However, it is not straightforward to distinguish magnetite (Fe_3O_4) from maghemite (γ-Fe_2O_3) using electron diffraction patterns. Therefore, direct information on the NPs phase composition is provided by powder XRD, where two major phases are identified: spinel iron oxide (Fe_3O_4 JCPDF # 85-1436 and/or γ-Fe_2O_3 JCPDF # 39-1346) and FeO (JCPDF #77-2355) and (see Fig. 1(d)). The only plausible core–shell structure would be a FeO core coated by spinel iron oxide shell and such a structure could arise due to metastability of the FeO phase. Both wüstite and spinel type iron oxide phases such as Fe_3O_4 and γ-Fe_2O_3 have an FCC oxygen sublattice and hence yields similar diffraction patterns, however their major peaks have somewhat different positions. Here we would like to mention that the dominating phase in the present case is spinel Fe_3O_4 phase with minor peaks of wüstite around the major one. Indeed, the positions of main reflections (3 1 1), (4 4 0) and (4 0 0) of the spinel phase and (1 1 1), (2 2 0) and (2 0 0) of the wüstite phase are too close, therefore the presence of FeO phase could not only determined on the basis of SAED pattern. The presence of spinel Fe_3O_4 and wüstite phase is further examined through magnetization versus temperature data as presented in the next section. Our results are in complete agreement with the results reported by Chen et al. [3] for the partially oxidized NPs of monodisperse FeO after 10 days. However, in the present work the core–shell structure remains intact even after a period of 125 days, whereas, they have observed the complete oxidation of wüstite phase into magnetite after a period of 120 days. The reason behind this disagreement is not clear yet at this stage, but we believe that the partial oxidation process may also strongly influenced by various synthesis conditions, the starting metallic precursor as well as washing/handling procedure. The difference between the current synthesis and the recipe proposed by Chen et al. [3] for the preparation of FeO NPs is probably due to use of different solvent/surfactant as well as starting metallic precursor.

The magnetization hystersis loops recorded at 2 K and 300 K in zero field cooling (ZFC) and field cooled (FC) mode in a field of 30 kOe from 350 K. At 300 K, the sample shows zero coecivity and retentivity, indicating that the particles are in SPM state (see inset (b) in Fig. 2) without saturation up to a field of 70 kOe, whereas at 2 K, the coercivity is ~2.5 kOe (ZFC mode) with high field of irreversibilty >50 kOe. Moreover, the loops in both ZFC and FC conditions cannot be actually saturated even in a high field of 140 kOe. These are the clear indication of strong internal interaction and co-existence of different magnetic phases into the individual particles. Therefore, this particular structure will create exchange bias (H_{EB}) field below the Neel temperature, T_N of FeO core [24].

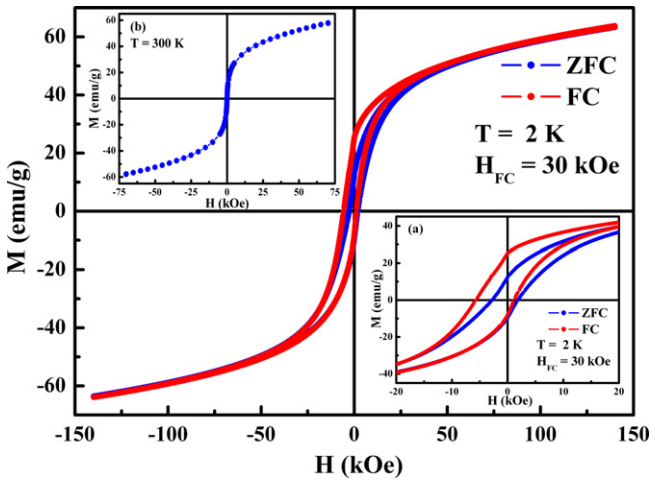

Fig. 2. Hysteresis loops taken in ZFC and FC modes at 2 K. Inset (a) showing the corresponding low field region, (b) hysteresis curve taken at 300 K.

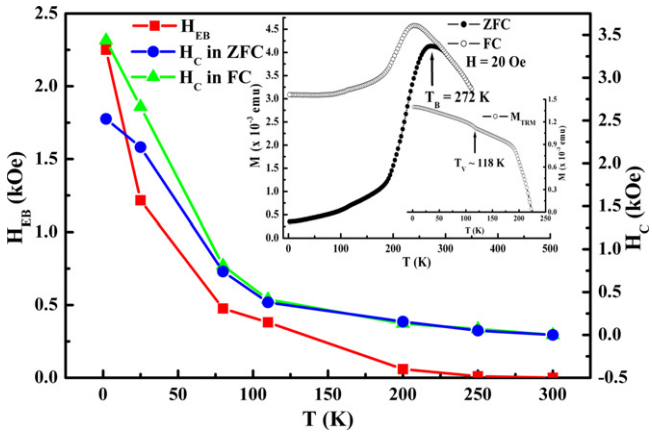

Fig. 3. Temperature-dependence of H_{EB} and H_C measured both in ZFC and FC mode. Inset showing the M vs. T curves taken in ZFC, FC and TRM modes.

Upon field cooling of sample from 350 K to temperature below the T_N of FeO (~200 K), the magnetic hystersis loop exhibits a set of interesting and unique features arising from the strong interfacial exchange coupling between the AFM core and FiM shell (see Fig. 2). These are (i) H_{EB}, shift towards negative field axis, and (ii) increased coercivity after FC as compared to ZFC. Here the shift is quantified by exchange field parameters $H_{EB} = -(H_R + H_L)/2$, while coercivity (H_C) defined as $H_C = (H_R - H_L)/2$, H_R and H_L being the points where the loop intersects the field axis. The corresponding value of H_{EB} is ~2.3 kOe (at 2 K). Additionally, as compared to ZFC hysteresis loop measured at 2 K, the FC loop gives rise to an increased value of coercivity $H_C^{FC} \approx 3.4$ kOe, which is more than the corresponding value observed in the ZFC condition. However, all these effects disappear at T close to or above $T_N \sim 198$ K, where AFM core become paramagnetic.

Fig. 3 shows that the EB are gradually reduced as the measurement temperature is increased and for $T \geq 200$ K, it disappears completely. Alternatively, the coercivity still exhibits a reasonable value. The disappearance of H_{EB} can be explained in terms of T_N (~198 K) of the AFM wüstite phase. However, in comparison to the results of Chen et al. [3], we have observed a sharp temperature variation of H_{EB} and H_C, which is anticipated for the system having intermediate interparticle interaction effect, as reported by Lima et al. [23]. Therefore, structural features together with magnetization data consistently confirm a multi-phase system of wüstite–magnetite NPs. Another, major evidence for the presence of wüstite and magnetite phase in the present case is also accessible from insets of Fig. 3, where a temperature dependent ZFC–FC magnetizations clearly reveal that the T_N of the AFM phase is equal to FeO phase. The ZFC and FC magnetization curves are almost comparable: the magnetization increases almost linearly with the increasing temperature from 2 K to 190 K followed by a sharp increase up to $T_B = 272$ K in ZFC and 242 K in FC case. Above this, the magnetization in ZFC and FC modes decreases smoothly. The broad shape of ZFC–FC magnetization curves and the comparative high value of T_B or T_{IRR}, (temperature at which M_{ZFC} and M_{FC} split), are in good agreement with the fact of intermediate interparticle interaction effect and the related sharp temperature variation of H_C and H_{EB} values. Further, we have also recorded the thermoremanent magnetization (TRM) by cooling the sample from 350 K to 2 K in a small field of 20 Oe and then the field was turned off and the magnetization was measured on warming cycle. Clearly one can see a step or kink in the M_{TRM} value at $T \sim 118$ K, which is hallmark for the Verwey transition and indicative of the presence of Fe_3O_4 phase [25–28]. Further investigations are underway to fully understand the results and to see the supplementary effect of time evolution on the stability of core–shell structure and the magnetic

properties. A detailed analysis, however, is beyond the scope of this publication.

4. Conclusions

To summarize, we have reported the successful preparation and characterization of partially oxidized wüstite–magnetite core–shell NPs as confirmed from XRD, HR-TEM, SAED and dc magnetization data. Despite the fact that the organometallic synthesis of Fe-oxide NPs leads to the formation of chemically stable magnetite NPs, our method allows the formation of metastable wüstite NPs. Finally, after pasivation, it leads to the formation of chemically stable FeO/Fe_3O_4 core–shell NPs even after a period of 100 days. Field cooled hystersis measurements confirm a negative horizontal shift along the field axis. Temperature dependence of the H_{EB} gave a maximum value of 2.3 kOe at 2 K after FC mode in an applied field of 30 kOe, which is almost vanished for temperatures close to the Neel temperature of wüstite phase (i.e., $T > 200$ K). The presence of H_{EB} is explained by the existence of a strong internal interaction at the interface of wüstite–spinel magnetite phase.

Acknowledgements

The authors are grateful to FAPESP (06/06792-2) and CNPq (Brazil) for providing financial support. We would also like to thank LNLS, Brazil for TEM imaging.

References

[1] B.Z. Zeng, S. Sun, Adv. Funct. Mater. 18 (2008) 391.
[2] Y. Hou, Z. Xu, S. Sun, Angew. Chem. Int. Ed. 46 (2007) 6329.
[3] C.J. Chen, R.K. Chiang, H.Y. Lai, C.R. Lin, J. Phys. Chem. C 114 (2010) 4258.
[4] W.H. Meiklejohn, C.P. Bean, Phys. Rev. 105 (1957) 904.
[5] C. Chappert, A. Fert, F.N. Van Dau, Nat. Mater. 200 (1999) 552.
[6] V. Skumryev, S. Stoyanov, Y. Zhang, G. Hadjipanyis, D. Givord, J. Nogues, Nature (London) 423 (2003) 850.
[7] Q.K. Ong, A. Wei, Xiao-M. Lin, Phys. Rev. B 80 (2009) 134418.
[8] S. Guo, W. Liu, M. Meng, X.H. Liu, W.J. Gong, Z. Han, Z.D. Zhang, J. Alloys Compd. 497 (2010) 10.
[9] H.T. Hai, H.T. Yang, H. Kura, D. Hasegawa, Y. Ogata, M. Takahashi, T. Ogawa, J. Colloid Interface Sci. 346 (2010) 37.
[10] T. Tsuzuki, F. Schäffel, M. Muroi, P.G. McCormick, J. Alloys Compd. 509 (2011) 5420.
[11] M.P. Fernández-García, P. Gorria, M. Sevilla, A.B. Fuertes, J.M. Greneche, J.A. Blanco, J. Alloys Compd., doi:10.1016/j.jallcom.2010.12.206.
[12] K. Karthik, G.K. Selvan, M. Kanagaraj, S. Arumugam, N. Victor Jaya, J. Alloys Compd. 509 (2011) 181.
[13] J. Nogués, I.K. Schuller, J. Magn. Magn. Mater. 192 (1999) 203.
[14] A.E. Berkowitz, K. Takano, J. Magn. Magn. Mater. 200 (1999) 552.
[15] R.L. Stamps, J. Phys. D: Appl. Phys. 33 (2000) R247.
[16] J. Nogués, J. Sort, V. Langlais, S. Doppiu, B. Dieny, J.S. Munoz, S. Surinach, M.D. Baro, S. Stoyanov, Y. Zhang, Int. J. Nanotechnol. 2 (2005) 23.
[17] J.F. Bobo, L. Gabillet, M. Bibes, J. Phys.: Condens. Matter 16 (2004) S471.
[18] R.K. Zheng, G.H. Wen, K.K. Fung, X.X. Zhang, J. Appl. Phys. 95 (2004) 5244.
[19] L.D. Bianco, D. Fiorani, A.M. Testa, E. Bonetti, L. Signorini, Phys. Rev. B 70 (2004) 052401.
[20] D.W. Kavich, J.H. Dickerson, S.V. Mahajan, S.A. Hasan, J.H. Park, Phys. Rev. B 78 (2008) 174414.
[21] M.S. Sheera, P. Roy, M. Manivannan, Mater. Res. Soc. Symp. Proc. 581 (2000) 511.
[22] R.H. Kodama, A.E. Berkowitz, E.J. McNiff Jr., S. Foner, J. Appl. Phys. 81 (1997) 5552.
[23] E. Lima Jr., J.M. Vargas, H.R. Rochenberg, R.D. Zysler, J. Nanosci. Nanotechnol. 8 (2008) 5913.
[24] A. Shavel, B.R. Gonzalez, M. Spasova, M. Spasova, M. Farle, L.M. Liz-Marzan, Adv. Mater. 17 (2007) 3870.
[25] R. Prozorov, T. Prozorov, S.K. Mallapragada, B. Narasimhan, T.J. Williams, D.A. Bazylinski, Phys. Rev. B 76 (2007) 054406.
[26] J. Garcia, G. Subias, J. Phys.: Condens. Matter 16 (2004) R145.
[27] F. Walz, J. Phys.: Condens. Matter 14 (2002) R285.
[28] E.J. Verwey, Nature 144 (1999) 327.